Hybrid Raman/fiber Bragg grating sensor for distributed temperature and discrete dynamic strain measurements

Iacopo Toccafondo,* Mohammad Taki, Alessandro Signorini, Farhan Zaidi, Tiziano Nannipieri, Stefano Faralli, and Fabrizio Di Pasquale

Scuola Superiore Sant'Anna, via G. Moruzzi 1, Pisa 56124, Italy
**Corresponding author: i.toccafondo@sssup.it*

Received July 30, 2012; revised September 17, 2012; accepted September 17, 2012;
posted September 18, 2012 (Doc. ID 173424); published October 22, 2012

We propose and experimentally demonstrate a hybrid fiber optic sensing technique that effectively combines Raman optical time domain reflectometry and in-line time-division-multiplexing for fiber Bragg grating (FBG) dynamic interrogation. The highly integrated proposed scheme employs broadband apodized low reflectivity FBGs with a single narrowband optical source and a shared receiver block, allowing for simultaneous measurements of distributed static temperature and discrete dynamic strain, over the same sensing fiber. © 2012 Optical Society of America

OCIS codes: 060.2370, 230.1480, 280.1350, 280.4788, 290.5860.

Fiber optic sensing of physical parameters like temperature and strain are fundamentally based on two alternative approaches [1,2]: distributed sensing, in which the measurand is continuously and quasi-statically sensed along the optical fiber exploiting Rayleigh, Raman, and Brillouin scattering effects, and discrete or point sensing, where the measurand is obtained at specific fiber locations only, allowing however dynamic measurements using, for instance, fiber Bragg gratings (FBGs).

To date, Raman-based distributed temperature sensing (RDTS) is the most successful and widely used technology for distributed measurements [2]. On the other hand, FBGs are widely employed devices for performing multiplexed discrete optical sensing of several physical parameters, including pressure, humidity, magnetic, and electric fields [3,4].

Several application fields, such as industrial plant monitoring and microleakage detection in oil and gas wells and pipelines, would strongly benefit from simultaneous measurements of both distributed temperature and discrete dynamic strain. The slow temperature profiling throughout a large industrial plant or a pipeline, together with dynamic vibration information at some specific critical points, can effectively detect anomalous operating conditions (i.e., overheating, leakages, and fire) and simultaneously provide dynamical monitoring of the structure's condition. The need for measuring distributed static temperature and/or strain, simultaneously with discrete dynamic strain at some specific critical points can open new research directions in the optical fiber sensing field [5].

In this Letter we propose a highly integrated hybrid sensing system that effectively combines the advantages of both RDTS and FBG-based dynamic sensing, allowing for simultaneous distributed temperature sensing and dynamic discrete strain measurements using a single mode optical fiber, a common pulsed narrowband optical source, and a shared receiver unit.

In RDTS systems, light pulses are launched into the sensing fiber generating spontaneous Raman scattering (SpRS), which is measured using the optical time-domain reflectometry (OTDR) technique [2]. The intensity of the anti-Stokes SpRS light component strongly depends on the fiber temperature. In order to distinguish real temperature changes from local fiber loss variations or laser source power fluctuations, normalization with a temperature-independent OTDR trace, such as Stokes SpRS or Rayleigh, must be performed [4]. On the other hand, FBGs are point fiber-sensing devices acting as band-reflect filters whose Bragg wavelength (λ_B) shifts linearly with local temperature and strain due to changes in the effective index and grating pitch [2].

The hybrid sensing approach proposed in this Letter makes use of a single pulsed laser for both Raman and FBG sensing whose interrogation technique for dynamic strain measurement is illustrated in Fig. 1.

A single pulsed narrowband pump laser is used to interrogate a pair of Gaussian apodized FBGs, placed close to each other in each sensing point, both characterized by low reflectivity and a broadband spectrum. As schematically shown in Fig. 1, the two reflected spectra from the FBGs within the same sensing point are symmetrically shifted with respect to the central wavelength of the laser source. The proposed interrogation technique exploits the FBG pair as reflective linear filters to translate wavelength shift into amplitude variation. In particular, considering the Gaussian reflectivity profiles of the employed FBGs, the following interrogation function $\rho(\Delta\lambda_B)$ is defined:

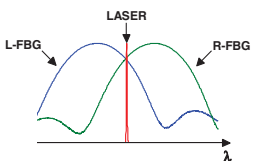

Fig. 1. (Color online) Optical spectrum of the proposed dynamic strain interrogation technique.

0146-9592/12/214434-03$15.00/0

$$\rho(\Delta\lambda_B) = \ln\left(\int_{Z_{\text{L-FBG}}}^{Z_{\text{L-FBG}}+\Delta Z} I_{\text{LR-FBG}}(\Delta\lambda_B,\xi)\mathrm{d}\xi\right) - \ln\left(\int_{Z_{\text{R-FBG}}}^{Z_{\text{R-FBG}}+\Delta Z} I_{\text{LR-FBG}}(\Delta\lambda_B,\xi)\mathrm{d}\xi\right), \quad (1)$$

where L-FBG and R-FBG stand for left and right FBG in the pair. $I_{\text{LR-FBG}}(\Delta\lambda_B,\xi)$ is the back-reflected intensity trace from the two FBGs, which is dependent on the Bragg wavelength shift $\Delta\lambda_B$; $Z_{\text{L-FBG}}$ and $Z_{\text{R-FBG}}$ are the longitudinal positions of the FBGs; and ΔZ is the spatial extension of the FBGs' response. It is worth noting that using the ratio of back-reflected intensities from both FBGs can provide immunity to fiber losses and laser power fluctuations as well as good linearity over a large sensing range (depending on the spectral separation between L-FBG and R-FBG) [5].

The experimental setup of the proposed Raman-FBG sensor is schematically shown in Fig. 2.

A narrow-band pulsed laser operating at 1550.50 nm, followed by a variable optical attenuator (VOA), is used to generate, at a repetition rate of 8.33 kHz, pump pulses of 33 dBm peak power and a pulse-width of 10 ns, providing 1 m spatial resolution, considering chromatic dispersion in single mode fibers (SMFs) is negligible. The generated pulses are launched into the sensing fiber through an optical circulator, which also couples the back-reflected light to a 4-port filter used to separate the Raman anti-Stokes, Raman Stokes, and Rayleigh bands. The receiver block consists of two avalanche photodiodes for anti-Stokes and Stokes light detection and a PIN photodiode for the FBG back-reflected light intensity measurement. The detected lights are then sent to a multi-channel 8 bit analog-to-digital converter (ADC) with 1 GS /s sampling frequency (to ensure an accurate reconstruction of the FBG's shape) for simultaneously acquiring the analog waveforms. The fiber under examination is composed by 10.9 km of single mode fiber and two sensing points located at 0.5 km and 10.7 km, respectively. Each sensing point consists of a pair of FBGs with 1% nominal reflectivity and a 2.5 nm line-width centered at different wavelengths (L-FBG at 1549.50 nm and R-FBG at 1551.50 nm).

Figure 3 shows an example of an acquired anti-Stokes trace at room temperature, where we can clearly observe the peaks at the spatial locations corresponding to the position of the gratings (the insets in Fig. 3 clearly shows two peaks corresponding to the two FBGs in each sensing point). Each peak is generated by the corresponding

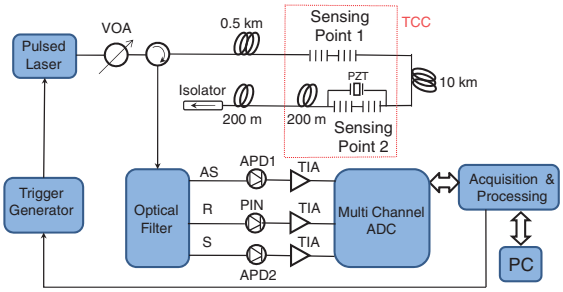

Fig. 2. (Color online) Experimental setup of the hybrid Raman/FBG sensor.

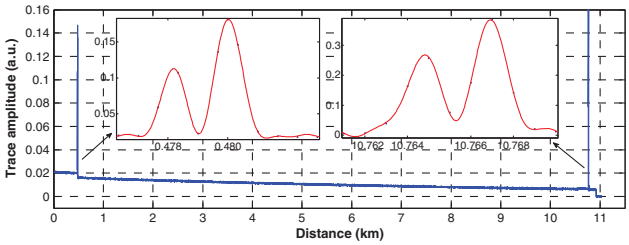

Fig. 3. (Color online) Raman anti-Stokes trace at room temperature.

FBG, which creates a reflected pump pulse at 1550.5 nm back-propagating to the fiber input while generating anti-Stokes scattering. The forward component of this scattering co-propagates with the reflected pulse to the fiber input while accumulating energy, which finally results in energy peaks at the corresponding FBG positions. These peaks are superimposed to the standard back-scattered Raman anti-Stokes trace. Similar peaks are also present in the Stokes SpRS trace generated at each position of the fiber by the same mechanism. As can be clearly seen in Fig. 3, the second sensing point returns higher power peaks, since the forward scattering, induced by FBGs reflection in the counter-propagating direction with respect to the pump, is summed over a much longer distance. Nevertheless, these peaks do not affect the distributed temperature measurement, which can be accurately performed along the whole sensing fiber, with the obvious exception being in close proximity of the FBGs, where we are only interested in dynamic strain measurements.

In order to analyze and validate the capability of our sensor to perform static distributed temperature and discrete dynamic strain measurements simultaneously, we placed the FBGs of both sensing points together with 200 m of SMF (preceding the second sensing point) inside a temperature-controlled chamber (TCC). In addition, the two FBGs of the sensing point located at 10.7 km have been glued to a piezoelectric actuator (PZT) driven by a waveform generator. The FBG responses of both sensing points have been first statistically characterized as a function of temperature by setting the TCC at different values and acquiring the time-domain traces of the back-reflected signals. For a complete FBG characterization, 100 traces were averaged for each TCC temperature, and the interrogation function was then calculated. As expected, comparing the linear fitting (solid line) with the experimental data (square dots) in Fig. 4(a), confirms a linear behavior of the interrogation function versus temperature. The amplitude variations of the back-reflected pulses from L-FBG and R-FBG due to temperature

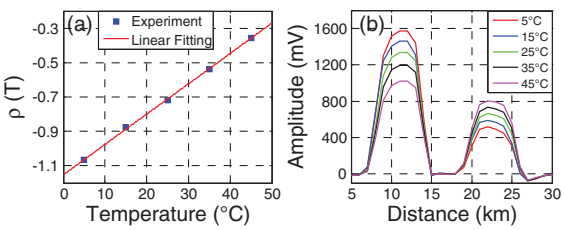

Fig. 4. (Color online) (a) Characterization of the interrogation function against applied temperature and (b) reflected pulse intensity from both FBGs at different temperatures.

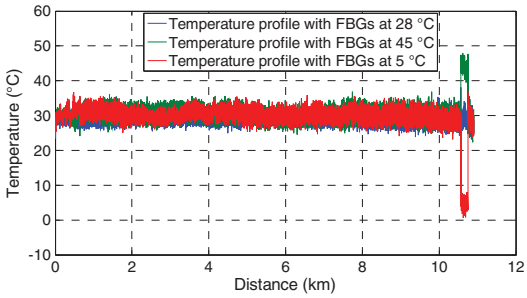

Fig. 5. (Color online) Temperature profile along 10.9 km of fiber.

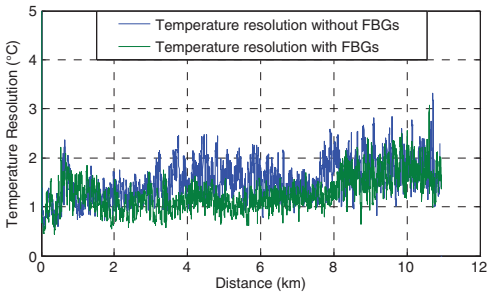

Fig. 6. (Color online) Temperature resolution along the fiber for the setup with (green) and without (blue) FBGs.

changes are reported in Fig. 4(b). It is worth noting that, although the interrogation function is used to map both strain and temperature values, dynamic strain variations can be extracted using high-pass filtering, thus removing the static component of the signal.

In order to study the influence of the FBG-based sensing points on the distributed temperature measurements, Raman-based temperature measurements were carried out setting the TCC temperature at three different values: 5°C, 28°C, and 45°C, respectively. The temperature profiles, estimated at each different temperature and reported in Fig. 5, clearly appear undistorted. We can evidently note that the FBGs at the two sensing points, ~0.5 km and ~10.7 km distances, have no influence on the Raman temperature measurement. To fully demonstrate the robustness of our hybrid sensor system, excluding possible spurious effects of the FBGs on the RDTS performance, distributed temperature measurements at 28°C have been repeated under the same conditions using the same optical fiber spools without splicing the FBG-point sensors. The corresponding temperature resolutions with and without FBGs have been calculated from the standard deviation of the measured temperatures and are shown in Fig. 6. We can see consistent results in both cases, with a similar trend in the resolution versus distance, fully demonstrating that FBG sensing points have no impact on the Raman

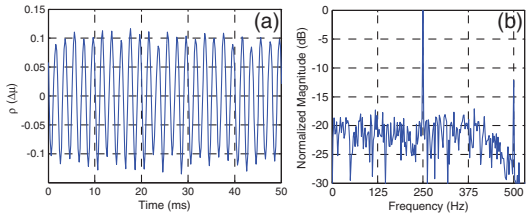

Fig. 7. (Color online) Dynamic strain measurements at 250 Hz. (a) Time-domain trace and (b) normalized fast Fourier transform.

temperature measurements. The worst temperature resolution (~10.8 km distance) is calculated to be ~2°C.

Finally, dynamic strain measurements have been carried out by applying a sinusoidal strain waveform (~410 με peak-to-peak) to the PZT actuator on the sensing point, at a distance of ~10.7 km. The waveform frequency and the TCC temperature have been changed to evaluate the dynamic sensing capabilities of the system under different conditions. Figure 7(a) shows a dynamic strain acquisition at room temperature with a 250 Hz sinusoidal input waveform of the PZT actuator; the acquired time-domain dynamic strain trace is in good agreement with the (known) applied strain waveform. The normalized fast Fourier transform of the measured trace is shown in Fig. 7(b); as we can see, the fundamental component is easily identified among other spurious spectral components, with a power lower than 10 dB. Similar traces were obtained at different TCC temperatures and frequencies. The dynamic strain resolution was estimated to be ~60 $n\varepsilon/(\mathrm{Hz})^{1/2}$ at 250 Hz.

A hybrid Raman/FBG sensor system using a highly integrated interrogation unit (sharing a narrowband pulsed source, the sensing fiber, and the receiver stage) has been implemented. The experimental results show simultaneous distributed sensing capabilities with temperature resolution of 2°C at 10.9 km and dynamic sensing with discrete FBG dynamic strain resolution of ~60 $n\varepsilon/(\mathrm{Hz})^{1/2}$ at 250 Hz, enabling the use of such a simple and effective hybrid technique in many applications where distributed temperature and discrete dynamic strain measurements are simultaneously required.

References

1. N. Anscombe and O. Graydon, Nat. Photonics **2**, 143 (2008).
2. K. T. V. Grattan and T. Sun, Sens. Actuators A **82**, 40 (2000).
3. A. D. Kersey, M. A. Davis, H. J. Patrick, M. LeBlanc, and K. P. Koo, J. Lightwave Technol. **15**, 1142 (1997).
4. J. P. Dakin and D. J. Pratt, IEEE Electron. Lett. **21**, 569 (1985).
5. T. Nannipieri, M. Taki, F. Zaidi, A. Signorini, M. A. Soto, G. Bolognini, and F. Di Pasquale, "Hybrid BOTDA/FBG sensor for discrete dynamic and distributed static strain/temperature measurements," presented at the 22nd International Conference on Optical Fiber Sensors (OFS-22), October 15–19, 2012, Beijing, China, paper no. 8421-205.